# Explicit Backstepping Kernel Solutions for Leak Detection in Branched Pipe Flows

Nils Christian A. Wilhelmsen and Ole Morten Aamo

***Abstract*— Explicit solutions are given for a set of $n+m$ linear hyperbolic observer backstepping kernel equations used for leak detection in branched pipe flows. It is identified that the kernel equations can be separated into $N+1$ distinct Goursat problems for $2(j+1)$ coupled PDEs each, $j \in \{0,1,\ldots,N\}$ and $N+1$ being the number of pipes connected via the branching point. Expressing the solutions as infinite matrix power series, the solution to each set of equations is shown to depend on a simplified, scalar Goursat problem, the solution of which is given in terms of derivatives of a modified Bessel function of the first kind. Furthermore, it is shown that the infinite matrix power series expressing the solution writes in terms of modified Bessel functions of the first kind and Marcum Q-functions, as is the case for the previously solved $2\times 2$ constant coefficient case. A numerical example showing adaptive observer gains for leak detection computed via the explicit solutions for multiple operating points of a branched pipe flow is given to illustrate the results.**

## I. INTRODUCTION

### A. Background

Techniques for automatically finding leaks range from camera-based inspection using local [1] or satellite imagery [2], methods relying on hardware such as fibre-optic cables [3] or ultrasonic flow monitors [4] being installed along the pipelines, to software-based methods that find leaks by processing signals from a limited number of sensors placed at strategic points in the pipeline system [5]. One promising approach in the latter class of methods is model-based leak detection, where mathematical models of physical variables of interest, such as pressure, flow or temperature are used as starting points for algorithm development. In [6], where a model-based leak detection methodology is proposed, it is argued that using transient (rather than static) models of the pipe flows allows the detection of significantly smaller leaks. A range of model-based contributions considering leak detection using state observer tools, such as [7], have followed.

As the field of control theory was at the time not ripe enough for the design of state observers based directly on distributed parameter models of the pipe flow, most initial contributions relied on discretizing the models in space to obtain finite-dimensional approximations on which algorithm design could be performed with available tools. This remained the case (apart from some heuristic contributions such as [8]) until [9], where the first distributed parameter state observer-based leak detection method with rigorous convergence guarantees was developed, relying on the development of the infinite-dimensional backstepping method for hyperbolic PDEs that appeared in [10].

To implement state observers designed via the backstepping approach, one is required to solve a particular set of PDEs, referred to as the *kernel equations*. In general these do not have any (known) closed-form solution, and must hence be approximated numerically. However, during the development of the backstepping method it was identified, initially for parabolic PDEs, that in certain (often simple) cases the kernel solutions could be expressed in closed form [11]. In [12] the kernel equations for $2\times 2$ linear hyperbolic PDEs with constant coefficients were solved in closed form, which is exploited in [9] for application to leak detection. In [13] explicit solutions are given for a $4\times 4$ system of kernel equations.

The methodology proposed for a single pipeline in [9], has later been extended to branched pipe flows in [14] and pipes connected in a ring structure in [15]. The associated kernel equations for these two respective designs are more complex, and due to the non-triviality of solving them and explicit solutions not being readily available in the literature, they have previously only been approximated numerically.

We extend here the results from [12] by offering exact analytical solutions to the kernel equations considered in [14]. The practical benefit to having explicit solutions of the kernel equations is most obvious in applications where the underlying system parameters are time-varying. For example, in practical water distribution systems the mean flow (and consequently also the friction factor) is varying as a function of time, based on the time of day and season of the year [16]. In [17] the observer from [9] is implemented for a nonlinear pipe flow model with varying levels of mean flow by calculating the observer gains as a function of the resultant friction factor through evaluating the explicit kernel solutions directly. Thus, having closed-form solutions facilitates the implementation of such an observer by removing the need to numerically approximate the full kernel solutions every time the operating point changes via a numerical algorithm, something which can be computationally burdensome.

Additionally, as the friction factor is typically an uncertain parameter, having explicit solutions opens up the possibility for adaptive approaches such as updating an estimate of the friction factor in closed loop together with the backstepping gains. Other practical benefits to having the explicit solutions at hand is the increased numerical accuracy at a cheap computational price, especially for systems with a large

The authors are with the Department of Engineering Cybernetics, Norwegian University of Science and Technology (NTNU), 7491 Trondheim, Norway.

E-mail: nils.c.wilhelmsen@ntnu.no (N.C.A. Wilhelmsen), aamo@ntnu.no (O.M. Aamo)

number of pipes in the branching point. Additionally it removes the need to implement software to approximate the kernels, which can be a time-consuming task. Furthermore, the explicit solutions we obtain can be useful as a benchmark to aid in the development of numerical methods for kernel equations similar to the ones considered here, but where explicit solutions are impossible to find.

### B. Problem statement

We consider here the same setup as considered in [14], namely $N+1$ pipelines of lengths $l_i$ and cross-sectional areas $A_i$, for $i \in \{0,1,2\ldots,N\}$ interconnected at a single branching point. The pressure $p_i$ and flow $q_i$ in pipe $i$ are assumed, for $z_i \in (0,l_i)$ and $t>0$, to be governed by (with the index on $z$ dropped for brevity)

$$\partial_t p_i(z,t) + \frac{\beta}{A_i}\partial_z q_i(z,t) = -\frac{\beta}{A_i} d_i(z)\chi_i \tag{1a}$$

$$\partial_t q_i(z,t) + \frac{A_i}{\rho}\partial_z p_i(z,t) = -\frac{F_i}{\rho} q_i(z,t) - A_i g \sin\phi_i(z) - \frac{\eta_i}{A_i} d_i(z)\chi_i \tag{1b}$$

where $\beta$ is the flow bulk modulus, $\rho$ is the density, $g$ is the gravitational constant, $F_i$ is the friction factor of pipe $i$ and $\phi_i$ is the inclination angle as a function of $z$. The leaks are characterized by the gross volumetric flow $\chi_i$ of all leaks out of pipe $i$, together with their (normalized) spatial distribution $d_i$ and factor $\eta_i \propto q_{i,0}$ (see [14], [18]), $q_{i,0}$ being the mean flow in pipe $i$.

The boundary conditions are given by

$$p_0(l_0,t) = p_{0,l_0}(t), \qquad q_i(l_i,t) = q_{i,l_i}(t) \tag{2a}$$

$$q_0(0,t) = -\sum_{j=1}^{n} q_j(0,t), \qquad p_i(0,t) = p_0(0,t) \tag{2b}$$

expressing the reservoir pressure $p_{0,l_0}$ to be imposed at $z = l_0$ for pipe 0, consumer demands $q_{i,l_i}$ be imposed at $z = l_i$ for pipes $i > 0$, in addition to uniqueness of pressure and continuity of flow in the branching point at $z = 0$.

It is shown in [14] that, under the assumption of pressure and flow measured at the pipe inlet and outlet boundaries only, the branched pipe flow system (1)–(2) can via an invertible change of coordinates be mapped into an equivalent system in Riemann coordinates. This system, defined in terms of distributed state vectors $u, v$, evolves over space and time $(x,t) \in [0,1]\times[0,\infty)$ according to

$$u_t(x,t) + \Lambda u_x(x,t) = C_1(x)v(x,t) \tag{3a}$$

$$v_t(x,t) - \Lambda v_x(x,t) = C_2(x)u(x,t) \tag{3b}$$

$$u(0,t) = Qv(0,t) + \kappa \tag{3c}$$

$$v(1,t) = Ru(1,t) + Bq_l(t) \tag{3d}$$

$$y(t) = u(1,t) \tag{3e}$$

where an unknown vector parameter $\kappa$ of dimension $N+1$ characterises possible leaks. The state vectors $u$, $v$ are each of dimension $N+1$ so that

$$u = \begin{bmatrix} u_0 & u_1 & \ldots & u_N \end{bmatrix}^\top, \quad v = \begin{bmatrix} v_0 & v_1 & \ldots & v_N \end{bmatrix}^\top.$$

The signals $q_l(t) = [q_0(l_0,t),\ldots,q_n(l_n,t)]^\top$ and $y(t)$ are measured, with $y(t)$ physically corresponding to a linear combination of the measured pressure and flow at $z = l$ (see [14] for the exact definition). The remaining system coefficients are assumed known, and defined as

$$\Lambda := diag\{\lambda_0,\lambda_1,\ldots,\lambda_N\}, \tag{4a}$$

$$C_j(x) := diag\{c_{0,j}(x), c_{1,j}(x),\ldots,c_{N,j}(x)\} \tag{4b}$$

$$Q := I_{N+1} - \frac{2}{A_T} a \mathbb{1}_{1\times(N+1)} \tag{4c}$$

$$R := -\exp(-2\cdot diag\{\gamma_0,\gamma_1,\ldots,\gamma_N\}) \tag{4d}$$

$$B := \exp(-diag\{\gamma_0,\gamma_1,\ldots,\gamma_N\}) \tag{4e}$$

in terms of physical parameters as

$$\lambda_i = \frac{1}{l_i}\sqrt{\frac{\beta}{\rho}}, \qquad \gamma_i = \frac{l_i F_i}{2\sqrt{\beta\rho}} \tag{5a}$$

$$c_{i,1}(x) = -\lambda_i\gamma_i e^{2\gamma_i x}, \qquad c_{i,2}(x) = -\lambda_i\gamma_i e^{-2\gamma_i x} \tag{5b}$$

$$a = \begin{bmatrix} A_0 & A_1 & \ldots & A_N \end{bmatrix}, \qquad A_T = \sum_{i=0}^{N} A_i. \tag{5c}$$

It is assumed, without loss of generality, that the transport speeds are ordered as

$$\lambda_0 \le \lambda_1 \le \cdots \le \lambda_N.$$

*Remark 1.1:* Although we develop the explicit solutions for the particular branched pipeline system (1)–(2) written in Riemann coordinates (3)–(5), the developed methodology can, with minor modifications, be applied to a wide range of applications modelling wave propagation in a network topology, including (but not limited to) electrical transmission lines [19] and traffic flow [20]. In particular, it is only necessary that the coupling matrices $C_1$, $C_2$ are diagonal and defined so that each coupled pair of PDEs can be mapped to a form with constant coupling coefficients, and all upper-left submatrices of $Q$ must be diagonalizable. However, the transport speeds $\Lambda$ for $u$ and $v$ may be different (but constant), and $R$, $B$ as well as signals $\kappa$, $q_l$ are irrelevant for the kernel solutions.

An adaptive observer is designed in [14] to produce estimates $\hat{u}$, $\hat{v}$ and $\hat{\kappa}$ of the unknown states $u$,$v$ and parameter $\kappa$, using the signals $q_l$, $y$. The observer reads

$$\hat{u}_t(x,t) + \Lambda\hat{u}_x(x,t) = C_1(x)\hat{v}(x,t) + P_1(x)(y(t) - \hat{u}(1,t)) \tag{6a}$$

$$\hat{v}_t(x,t) - \Lambda\hat{v}_x(x,t) = C_2(x)\hat{u}(x,t) + P_2(x)(y(t) - \hat{u}(1,t)) \tag{6b}$$

$$\hat{u}(0,t) = Q\hat{v}(0,t) + \hat{\kappa}(t) \tag{6c}$$

$$\hat{v}(1,t) = Ry(t) + Bq_l(t) \tag{6d}$$

$$\dot{\hat{\kappa}}(t) = L(y(t) - \hat{u}(1,t)) \tag{6e}$$

with $P_1$, $P_2$ distributed observer matrix gains and $L$ an adaptive matrix gain. To define these gains, introduce the kernel equations (originally introduced in [21])

$$\Lambda M_x^\alpha(x,\xi) + M_\xi^\alpha(x,\xi)\Lambda = C_1(x)M^\beta(x,\xi) \tag{7a}$$

$$-\Lambda M_x^\beta(x,\xi) + M_\xi^\beta(x,\xi)\Lambda = C_2(x)M^\alpha(x,\xi) \tag{7b}$$

$$\Lambda M^\alpha(x,x) - M^\alpha(x,x)\Lambda = 0 \tag{7c}$$

$$\Lambda M^\beta(x,x) + M^\beta(x,x)\Lambda = C_2(x) \tag{7d}$$

$$M^\alpha(0,\xi) - QM^\beta(0,\xi) = \Pi(\xi) \tag{7e}$$

$$m_{ij}^\alpha(x,1) = 0, \ 0 \le j < i \le N \tag{7f}$$

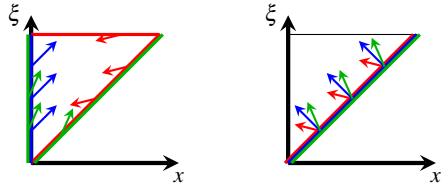


Fig. 1: Direction of characteristics and corresponding boundary conditions, depending on relative values of $i$ and $j$ (red for $j<i$, blue for $j=i$ and green for $j>i$). The characteristics of $m_{ij}^{\alpha}$ are shown to the left and the ones for $m_{ij}^{\beta}$ are to the right.

defining $(N+1)\times(N+1)$ matrix-valued functions

$$M^{\alpha}(x,\xi)=\{m_{ij}^{\alpha}(x,\xi)\}_{0\le i,j\le N}$$
$$M^{\beta}(x,\xi)=\{m_{ij}^{\beta}(x,\xi)\}_{0\le i,j\le N}$$

over the upper-triangular domain $\mathscr{T}=\{(x,\xi)|0\le x\le\xi\le 1\}$. The boundary condition (7f) is artificial and added to reduce discontinuities and ensure well-posedness of the solutions (see [21]). The matrix $\Pi=\{\varpi_{ij}\}_{1\le i,j\le N}$ is strictly lower triangular with elements

$$\varpi_{ij}(\xi)=\begin{cases}0, & \text{if } 0\le i\le j\le N\\ m_{ij}^{\alpha}(0,\xi)-\sum_{k=0}^{N}Q_{ik}m_{kj}^{\beta}(0,\xi) & \text{if } 0\le j<i\le N,\end{cases}$$

where $Q_{ik}$ denotes the element in the $i^{th}$ row and $k^{th}$ column of $Q=\{Q_{ik}\}_{0\le i,k\le N}$. It is shown in [14] that convergence of the estimates $\hat{u},\hat{v},\hat{\kappa}$ in (6) to their respective true values $u,v,\kappa$ in (3) is guaranteed by choosing $P_1$, $P_2$ as

$$P_1(x)=M^{\alpha}(x,1)\Lambda-\int_x^1 M^{\alpha}(x,\xi)d\xi F^{\alpha}L-F^{\alpha}L \tag{8a}$$

$$P_2(x)=M^{\beta}(x,1)\Lambda-\int_x^1 M^{\beta}(x,\xi)d\xi F^{\alpha}L \tag{8b}$$

and $L$ so that $LF^{\alpha}$ is Hurwitz, where

$$F^{\alpha}=\left(I_{N+1}+\int_0^1\Pi(\xi)d\xi\right)^{-1}$$

with $I_{N+1}$ denoting the $(N+1)\times(N+1)$ identity matrix.

Following similar steps to [12] and, as done in [9], exploiting structural properties of (7) specific to the application considered, we solve in the following for the kernels $M^{\alpha},M^{\beta}$ explicitly in closed form. To the best of the authors' knowledge, this is the first closed-form solution to backstepping kernels for an $n+m$ system of linear hyperbolic PDEs.[1]

## II. SIMPLIFICATION OF KERNEL EQUATIONS

Writing (7a)–(7b) out componentwise, we obtain $(N+1)^2$ pairs of PDEs independently coupled in-domain over the interior of $\mathscr{T}$, taking the form

$$\lambda_i\partial_x m_{ij}^{\alpha}(x,\xi)+\lambda_j\partial_\xi m_{ij}^{\alpha}(x,\xi)=c_{i1}(x)m_{ij}^{\beta}(x,\xi) \tag{9a}$$

$$-\lambda_i\partial_x m_{ij}^{\beta}(x,\xi)+\lambda_j\partial_\xi m_{ij}^{\beta}(x,\xi)=c_{i2}(x)m_{ij}^{\alpha}(x,\xi) \tag{9b}$$

with $i,j\in\{0,1,\dots,N\}$. The various pairs $m_{ij}^{\alpha},m_{ij}^{\beta}$ may, however, have couplings between each other via the boundary conditions (7c)–(7e). Writing the boundary conditions out explicitly and considering the directions of the characteristics (see Figure 1), we can identify three different cases.

[1]Here $n=m=N+1$.

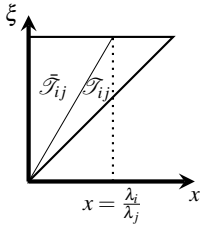


Fig. 2: Triangular domain $\mathscr{T}=\bar{\mathscr{T}}_{ij}\cup\mathscr{T}_{ij}$.

*1) $j<i$:*

$$m_{ij}^{\alpha}(x,x)=0,\qquad m_{ij}^{\alpha}(x,1)=0,\qquad m_{ij}^{\beta}(x,x)=0. \tag{10}$$

*2) $j=i$:*

$$m_{ii}^{\alpha}(0,\xi)=\sum_{k=0}^{N}Q_{ik}m_{ki}^{\beta}(0,\xi),\qquad m_{ii}^{\beta}(x,x)=\frac{c_{i2}(x)}{2\lambda_i}. \tag{11}$$

*3) $j>i$:*

$$m_{ij}^{\alpha}(x,x)=0,\qquad m_{ij}^{\alpha}(0,\xi)=\sum_{k=0}^{N}Q_{ik}m_{kj}^{\beta}(0,\xi), \tag{12a}$$

$$m_{ij}^{\beta}(x,x)=0. \tag{12b}$$

Firstly, from (10) it is immediately seen that for $j<i$ we can conclude $m_{ij}^{\alpha}\equiv m_{ij}^{\beta}\equiv 0$ across $\mathscr{T}$. The remaining equations (9), (11) for $j=i$ and (9), (12) for $j>i$ can thus be identified as $N+1$ independent sets of respectively $2(j+1)$ kernel equations each, for $j\in\{0,1,\dots,N\}$. Considering also the boundary conditions (12) and the direction of the corresponding characteristics, we see that for $j>i$ we have

$$m_{ij}^{\alpha}(x,\xi)=m_{ij}^{\beta}(x,\xi)=0,\ \text{for } (x,\xi)\in\mathscr{T}_{ij} \tag{13}$$

where the domain $\mathscr{T}_{ij}\subseteq\mathscr{T}$ is defined as the union $\mathscr{T}_{ij}=\mathscr{T}_{ij}^{l}\cup\mathscr{T}_{ij}^{r}$ of sub-domain $\mathscr{T}_{ij}^{l}=\{(x,\xi)|x\le\xi\le\frac{\lambda_j}{\lambda_i}x,0\le x\le\frac{\lambda_i}{\lambda_j}\}$ located to the left of $x=\frac{\lambda_i}{\lambda_j}$ and $\mathscr{T}_{ij}^{r}=\{(x,\xi)|x\le\xi\le 1,\frac{\lambda_j}{\lambda_i}\le x\le 1\}$ to the right (see Figure 2).

Since the kernels are only coupled in-domain in pairs and otherwise via the boundaries along the $\xi$-axis at $x=0$, we define the scaled kernels

$$\bar{m}_{ij}^{\alpha}(x,\xi)=m_{ij}^{\alpha}\left(\frac{\lambda_i}{\lambda_j}x,\xi\right),\quad \bar{m}_{ij}^{\beta}(x,\xi)=-m_{ij}^{\beta}\left(\frac{\lambda_i}{\lambda_j}x,\xi\right), \tag{14}$$

valid for[2] $\bar{\mathscr{T}}_{ij}=\{(x,\xi)|0\le\frac{\lambda_j}{\lambda_i}x\le\xi\le 1\}$.

Fixing an index $j\in\{0,1,\dots,N\}$, dividing both sides by $\pm\lambda_j$, using the definition of $c_{ik}$ from (5b) and defining the $(j+1)$-dimensional vector states $\bar{M}_j^{\alpha}=[\bar{m}_{0j}^{\alpha}\ \bar{m}_{1j}^{\alpha}\ \dots\ \bar{m}_{jj}^{\alpha}]^{\top}$, $\bar{M}_j^{\beta}=[\bar{m}_{0j}^{\beta}\ \bar{m}_{1j}^{\alpha}\ \dots\ \bar{m}_{jj}^{\beta}]^{\top}$, we have the $j+1$-dimensional vector Goursat problem

$$\partial_x\bar{M}_j^{\alpha}(x,\xi)+\partial_\xi\bar{M}_j^{\alpha}(x,\xi)=\Gamma_j^1(x)\bar{M}_j^{\beta}(x,\xi) \tag{15a}$$

$$-\partial_x\bar{M}_j^{\beta}(x,\xi)+\partial_\xi\bar{M}_j^{\beta}(x,\xi)=\Gamma_j^2(x)\bar{M}_j^{\alpha}(x,\xi) \tag{15b}$$

$$\bar{M}_j^{\alpha}(0,\xi)=\bar{Q}_j\bar{M}_j^{\beta}(0,\xi) \tag{15c}$$

$$\bar{M}_j^{\beta}(x,x)=\frac{\gamma_j}{2}e^{-2\gamma_j x}\mathbf{e}_{j+1} \tag{15d}$$

[2]Note that $\bar{\mathscr{T}}_{jj}=\mathscr{T}$.

where

$$\Gamma_j^1(x) = diag\left\{\frac{\lambda_0}{\lambda_j}\gamma_0 e^{2\gamma_0 x}, \frac{\lambda_1}{\lambda_j}\gamma_1 e^{2\gamma_1 x}, \ldots, \gamma_j e^{2\gamma_j x}\right\} \quad (16a)$$

$$\Gamma_j^2(x) = diag\left\{\frac{\lambda_0}{\lambda_j}\gamma_0 e^{-2\gamma_0 x}, \frac{\lambda_1}{\lambda_j}\gamma_1 e^{-2\gamma_1 x}, \ldots, \gamma_j e^{-2\gamma_j x}\right\}, \quad (16b)$$

the matrix

$$\bar{Q}_j := \{-Q_{ik}\}_{0\le i,k\le j} \quad (17)$$

is the $(j+1)\times(j+1)$ upper-left sub-matrix of $-Q$, and $\mathbf{e}_{j+1} = [0\ 0\ \ldots\ 0\ 1]^\top$.

We consider next in Section III-A the problem of finding the explicit solution to the Goursat problem (15) for any $j \in \{0,1,\ldots,N\}$, before recovering the solutions to (7) in Section III-B.

## III. SOLVING THE KERNELS

### A. Simplified kernels

To solve (15), similar to [12] we make the ansatz that the solutions can be expressed as infinite sums taking the form

$$\bar{M}_j^\alpha(x,\xi) = \sum_{n=0}^{\infty} \bar{Q}_j^n A_n(x,\xi), \quad \bar{M}_j^\beta(x,\xi) = \sum_{n=0}^{\infty} \bar{Q}_j^n B_n(x,\xi) \quad (18)$$

where $A_n$, $B_n$ are to be found. Substituting this assumed form into (15), it is straightforward to see that $A_n$, $B_n$ satisfy the set of equations

$$(\partial_x+\partial_\xi)A_n = \Gamma_j^1(x)B_n(x,\xi), \quad (-\partial_x+\partial_\xi)B_n = \Gamma_j^2(x)A_n(x,\xi) \quad (19a)$$

$$A_0(0,\xi) = 0, \qquad A_n(0,\xi) = B_{n-1}(0,\xi) \quad (19b)$$

$$B_0(x,x) = \frac{\gamma_j}{2}e^{-2\gamma_j x}\mathbf{e}_{j+1}, \qquad B_n(x,x) = 0. \quad (19c)$$

Since $\Gamma_j^1$, $\Gamma_j^2$ are diagonal matrices and the boundary conditions are defined element-wise, the set of equations (19) represent $j+1$ independent pairs of scalar equations. The equations for the first $j$ components have 0 at both boundaries at $n=0$, and recursively solving these for $n>0$ we see the solutions take the form

$$A_n(x,\xi) = \bar{a}_n(x,\xi)\mathbf{e}_{j+1}, \quad B_n(x,\xi) = \bar{b}_n(x,\xi)\mathbf{e}_{j+1} \quad (20)$$

with $\bar{a}_n, \bar{b}_n$ scalar functions. Let now

$$\hat{a}_n(x,\xi) = e^{\gamma_j(\xi-x)}\bar{a}_n(x,\xi), \quad \hat{b}_n(x,\xi) = e^{\gamma_j(\xi+x)}\bar{b}_n(x,\xi) \quad (21)$$

and scaling the domain $\hat{x} = \gamma_j x$, $\hat{\xi} = \gamma_j\xi$ and $a_n = \frac{2}{\gamma_j}\hat{a}_n$, $b_n = \frac{2}{\gamma_j}\hat{b}_n$, we have the scalar Goursat problem (for ease of readability the $\hat{}$ in $\hat{x},\hat{\xi}$ is omitted)

$$(\partial_x+\partial_\xi)a_n = b_n(x,\xi), \quad (-\partial_x+\partial_\xi)b_n = a_n(x,\xi) \quad (22a)$$

$$a_0(0,\xi) = 0, \qquad a_n(0,\xi) = b_{n-1}(0,\xi) \quad (22b)$$

$$b_0(x,x) = 1, \qquad b_n(x,x) = 0 \quad (22c)$$

over the scaled upper-triangular domain $\mathscr{T}_{\gamma_j} = \{(x,\xi) \mid 0 \le x \le \xi \le \gamma_j\}$. The solutions $(a_n,b_n)$ to (22) can be written explicitly as power series in a straightforward manner.

*Lemma 3.1:* The solutions $(a_n,b_n)$ to (22) are for $(x,\xi)\in\mathscr{T}_{\gamma_j}$ given by

$$a_n(x,\xi) = (\partial_x+\partial_\xi)^n\phi(x,\xi) \quad (23a)$$

$$b_n(x,\xi) = (\partial_x+\partial_\xi)^{n+1}\phi(x,\xi) \quad (23b)$$

with

$$\phi(x,\xi) = 2x\frac{\mathscr{I}_1(\sqrt{(-x+\xi)(x+\xi)})}{\sqrt{(-x+\xi)(x+\xi)}}, \quad (24)$$

and $\mathscr{I}_n$ denotes the modified Bessel function of the first kind of order $n$.

*Proof:* Mirroring (22) across the line $x=\xi$ by swapping $\xi\to x$, $x\to\xi$ and defining $\underline{a}_n(x,\xi) = a_n(\xi,x)$, $\underline{b}_n(x,\xi) = b_n(\xi,x)$, we have that they are defined over the lower-triangular domain $\mathscr{T}_{\gamma_j}^l = \{(x,\xi) \mid 0 \le \xi \le x \le \gamma_j\}$. Applying Lemmas 3.2 and A.1 from [12], the solution to $\underline{a}_n$, $\underline{b}_n$ is directly written as

$$\underline{a}_n(x,\xi) = (\partial_x+\partial_\xi)^n\bar{\phi}(x,\xi), \quad \underline{b}_n(x,\xi) = (\partial_x+\partial_\xi)^{n+1}\bar{\phi}(x,\xi)$$

in terms of $\bar{\phi}$ given by

$$\bar{\phi}(x,\xi) = 2\xi\frac{\mathscr{I}_1(\sqrt{(x+\xi)(x-\xi)})}{\sqrt{(x+\xi)(x-\xi)}}.$$

Mirroring back into the upper-triangular domain $\mathscr{T}_{\gamma_j}$, we obtain (23)–(24). ∎

Using Lemma A.2 from [12], $\phi$ in (24) is expanded as

$$\phi(x,\xi) = \sum_{k=0}^{\infty}\frac{(\frac{-x+\xi}{2})^k}{(k+1)!}\frac{(\frac{x+\xi}{2})^{k+1}}{k!} - \sum_{k=0}^{\infty}\frac{(\frac{-x+\xi}{2})^{k+1}}{(k+1)!}\frac{(\frac{x+\xi}{2})^k}{k!}, \quad (25)$$

and from Lemma 3.3 in [12] we have the $n^{th}$ order derivative

$$(\partial_x+\partial_\xi)^n\phi(x,\xi) = \sum_{k=0}^{\infty}\frac{\left(\frac{-x+\xi}{2}\right)^{k+n-1}}{(k+n-1)!}\frac{\left(\frac{x+\xi}{2}\right)^k}{k!} \times\left(1-\frac{\left(\frac{-x+\xi}{2}\right)^2}{(k+n)(k+n+1)}\right). \quad (26)$$

We introduce now two $(j+1)\times(j+1)$ matrix-valued functions $\Omega_j^\alpha$, $\Omega_j^\beta$. Let

$$\Omega_j^\alpha(x,\xi) := \frac{\gamma_j}{2}e^{\gamma_j(x-\xi)}\left\{I_{j+1}\sqrt{\frac{x+\xi}{-x+\xi}}\mathscr{I}_1(\gamma_j\sqrt{\xi^2-x^2}) + \bar{Q}_j^{-1}\mathscr{I}_0(\gamma_j\sqrt{\xi^2-x^2}) + (\bar{Q}_j-\bar{Q}_j^{-1})P_jS_j(x,\xi)P_j^{-1}\right\} \quad (27a)$$

$$\Omega_j^\beta(x,\xi) := \frac{\gamma_j}{2}e^{-\gamma_j(\xi+x)}\left\{\bar{Q}_j^{-1}\sqrt{\frac{-x+\xi}{x+\xi}}\mathscr{I}_1(\gamma_j\sqrt{\xi^2-x^2}) + \bar{Q}_j^{-2}\mathscr{I}_0(\gamma_j\sqrt{\xi^2-x^2}) + (I_{j+1}-\bar{Q}_j^{-2})P_jS_j(x,\xi)P_j^{-1}\right\}. \quad (27b)$$

with

$$P_j := \begin{bmatrix} -1 & -1 & \ldots & -1 & a_0/a_j \\ 1 & 0 & \ldots & 0 & a_1/a_j \\ 0 & 1 & \ldots & 0 & a_2/a_j \\ \vdots & \vdots & \ddots & \vdots & \vdots \\ 0 & 0 & \ldots & 0 & a_{j-1}/a_j \\ 0 & 0 & \ldots & 1 & a_j/a_j \end{bmatrix} \quad (28)$$

and

$$S_j(x,\xi) := diag\{\sigma(x,\xi)\ \sigma(x,\xi)\ \ldots\ \sigma(x,\xi)\ \sigma_j(x,\xi)\}. \quad (29)$$

The terms $\sigma$, $\sigma_j$ are defined as

$$\sigma(x,\xi) := e^{-\gamma_j\xi}\mathscr{Q}_1\left(\sqrt{\gamma_j(-x+\xi)}, \sqrt{\gamma_j(x+\xi)}\right) \quad (30)$$

$$\sigma_j(x,\xi) := e^{\frac{\gamma_j}{2}((\frac{1}{d_j}-d_j)x+(\frac{1}{d_j}+d_j)\xi)}$$

$$\times \mathscr{Q}_1\left(\sqrt{|d_j|\gamma_j(-x+\xi)}, \sqrt{\frac{\gamma_j}{|d_j|}}(x+\xi)\right), \quad (31)$$

where $\mathscr{Q}_1$ denotes the generalized Marcum Q-function of first order and $d_j := -1 + \frac{2}{A_T}\sum_{i=0}^{j} a_i$.

We will need the following technical Lemma, which is stated without proof due to lack of space.

*Lemma 3.2:* The matrix power series

$$\sum_{n=0}^{\infty} \bar{Q}_j^n \sum_{k=0}^{\infty} \frac{\left(\frac{\gamma_j}{2}(-x+\xi)\right)^{k+n}}{(k+n)!} \frac{\left(\frac{\gamma_j}{2}(x+\xi)\right)^{k}}{k!} = P_j S_j(x,\xi) P_j^{-1}. \quad (32)$$

We then have the following result.

*Lemma 3.3:* The solutions $\bar{M}_j^{\alpha}$, $\bar{M}_j^{\beta}$ to (15) are given by

$$\bar{M}_j^{\alpha}(x,\xi) = \Omega_j^{\alpha}(x,\xi)\mathbf{e}_{j+1} \quad (33a)$$

$$\bar{M}_j^{\beta}(x,\xi) = \Omega_j^{\beta}(x,\xi)\mathbf{e}_{j+1}. \quad (33b)$$

*Proof:* Applying Lemma 3.1, we can write

$$\bar{a}_n(x,\xi) = \frac{\gamma_j}{2} e^{\gamma_j(x-\xi)}(\partial_{\gamma_j x} + \partial_{\gamma_j \xi})^n \phi(\gamma_j x, \gamma_j \xi).$$

Substituting together with (20) into the assumed expression (18) for $\bar{M}_j^{\alpha}$ and using (25)–(26), we have

$$\begin{aligned}
&\bar{M}_j^{\alpha}(x,\xi) \\
&= \frac{\gamma_j}{2} e^{\gamma_j(x-\xi)} \Bigg\{ \bar{Q}_j^0 \sum_{k=0}^{\infty} \frac{\left(\frac{\gamma_j}{2}(-x+\xi)\right)^{k}}{(k+1)!} \frac{\left(\frac{\gamma_j}{2}(x+\xi)\right)^{k+1}}{k!} \\
&\quad + (\bar{Q}_j - \bar{Q}_j^{-1}) \sum_{n=0}^{\infty} \bar{Q}_j^n \sum_{k=0}^{\infty} \frac{\left(\frac{\gamma_j}{2}(-x+\xi)\right)^{k+n}}{(k+n)!} \frac{\left(\frac{\gamma_j}{2}(x+\xi)\right)^{k}}{k!} \\
&\quad + \bar{Q}_j^{-1} \sum_{k=0}^{\infty} \frac{\left(\frac{\gamma_j}{2}(-x+\xi)\right)^{k}}{k!} \frac{\left(\frac{\gamma_j}{2}(x+\xi)\right)^{k}}{k!} \Bigg\} \mathbf{e}_{j+1}.
\end{aligned}$$

Applying then Lemma 3.2 together with the identity ([22])

$$\sum_{k=0}^{\infty} \frac{\alpha^{k+n}}{(k+n)!} \frac{\beta^k}{k!} = \sqrt{\frac{\alpha^n}{\beta^n}} \mathscr{I}_n(2\sqrt{\alpha\beta}) \quad (34)$$

we obtain (33a). Performing similar steps for $\bar{M}_j^{\beta}$ yields (33b). ∎

### B. Main result

Lemma 3.3 is used together with the simplifications done in Section II to express the solutions of (7) in closed form. This is the main result of the paper.

*Theorem 3.4:* Denote by $\omega_j^{\alpha} = [\omega_{0,j}^{\alpha}\ \omega_{1,j}^{\alpha}\ \dots\ \omega_{j,j}^{\alpha}]^{\top}$, $\omega_j^{\beta} = [\omega_{0,j}^{\beta}\ \omega_{1,j}^{\beta}\ \dots\ \omega_{j,j}^{\beta}]^{\top}$ the rightmost (number $j+1$) column vector of respectively $\Omega_j^{\alpha}$, $\Omega_j^{\beta}$ in (27). The matrix-valued solutions $M^{\alpha}$, $M^{\beta}$ to (7) are upper triangular matrices given by

$$M^{\alpha}(x,\xi) = \begin{bmatrix} m_{0,0}^{\alpha}(x,\xi) & m_{0,1}^{\alpha}(x,\xi) & \dots & m_{0,N}^{\alpha}(x,\xi) \\ 0 & m_{1,1}^{\alpha}(x,\xi) & \dots & m_{1,N}^{\alpha}(x,\xi) \\ \vdots & \ddots & \ddots & \vdots \\ 0 & 0 & \dots & m_{N,N}^{\alpha}(x,\xi) \end{bmatrix} \quad (35a)$$

$$M^{\beta}(x,\xi) = \begin{bmatrix} m_{0,0}^{\beta}(x,\xi) & m_{0,1}^{\beta}(x,\xi) & \dots & m_{0,N}^{\beta}(x,\xi) \\ 0 & m_{1,1}^{\beta}(x,\xi) & \dots & m_{1,N}^{\beta}(x,\xi) \\ \vdots & \ddots & \ddots & \vdots \\ 0 & 0 & \dots & m_{N,N}^{\beta}(x,\xi) \end{bmatrix} \quad (35b)$$

where for $i \in \{0,1,\dots,j\}$, $j \in \{0,1,\dots,N\}$ we have

$$m_{i,j}^{\alpha}(x,\xi) = \begin{cases} \omega_{i,j}^{\alpha}(\frac{\lambda_j}{\lambda_i}x,\xi), & \text{if } (x,\xi) \in \bar{\mathscr{T}}_{ij} \\ 0, & \text{if } (x,\xi) \in \mathscr{T}_{ij} \end{cases} \quad (36a)$$

$$m_{i,j}^{\beta}(x,\xi) = \begin{cases} -\omega_{i,j}^{\beta}(\frac{\lambda_j}{\lambda_i}x,\xi), & \text{if } (x,\xi) \in \bar{\mathscr{T}}_{ij} \\ 0. & \text{if } (x,\xi) \in \mathscr{T}_{ij} \end{cases} \quad (36b)$$

*Proof:* Write $M^{\alpha} = [M_0^{\alpha}\ M_1^{\alpha}\ \dots\ M_N^{\alpha}]$, $M^{\beta} = [M_0^{\beta}\ M_1^{\beta}\ \dots\ M_N^{\beta}]$, where $M_j^{\alpha}$, $M_j^{\beta}$ denotes for $j \in \{0,1,\dots,N\}$ the $(j+1)^{th}$ column vector of respectively $M^{\alpha}$, $M^{\beta}$. Due to the boundary conditions (10) valid for $i \in \{j+1, j+2, \dots, N\}$, we have that $M_j^{\alpha}$, $M_j^{\beta}$ take the form

$$M_j^{\alpha}(x,\xi) = \begin{bmatrix} \mu_j^{\alpha}(x,\xi) \\ \mathbf{0}_{(N-j)\times 1} \end{bmatrix}, \quad M_j^{\beta}(x,\xi) = \begin{bmatrix} \mu_j^{\beta}(x,\xi) \\ \mathbf{0}_{(N-j)\times 1} \end{bmatrix} \quad (37)$$

where $\mu_j^{\alpha} = [m_{0j}^{\alpha}\ m_{1j}^{\alpha}\ \dots\ m_{jj}^{\alpha}]^{\top}$, $\mu_j^{\beta} = [m_{0j}^{\beta}\ m_{1j}^{\beta}\ \dots\ m_{jj}^{\beta}]^{\top}$ are column vectors of length $j+1$, and $\mathbf{0}_{(N-j)\times 1}$ denotes the column vector of length $N-j$ containing only zeros. This shows that $M^{\alpha}$, $M^{\beta}$ are upper triangular matrices as given in (35).

Next, using (13)–(14) we have that

$$m_{ij}^{\alpha}(x,\xi) = \begin{cases} \bar{m}_{ij}^{\alpha}(\frac{\lambda_j}{\lambda_i}x,\xi), & \text{if } (x,\xi) \in \bar{\mathscr{T}}_{ij} \\ 0, & \text{if } (x,\xi) \in \mathscr{T}_{ij} \end{cases} \quad (38a)$$

$$m_{ij}^{\beta}(x,\xi) = \begin{cases} -\bar{m}_{ij}^{\beta}(\frac{\lambda_j}{\lambda_i}x,\xi), & \text{if } (x,\xi) \in \bar{\mathscr{T}}_{ij} \\ 0, & \text{if } (x,\xi) \in \mathscr{T}_{ij}. \end{cases} \quad (38b)$$

From (33) in Lemma 3.3 it is straightforward to see that

$$\bar{M}_j^{\alpha}(x,\xi) = \omega_j^{\alpha}(x,\xi), \qquad \bar{M}_j^{\beta}(x,\xi) = \omega_j^{\beta}(x,\xi)$$

and substituting this element-wise into (38) we obtain (36). ∎

## IV. Numerical example

We demonstrate the results here on a numerical example. We use the closed-form kernel solutions from Theorem 3.4 to obtain the observer gains (8) for multiple different operating points of a branched pipe flow, using the same system parameters as used in Section 6 of [14]. This is to emphasize the use of the explicit kernel solutions in a gain-scheduling setting, where the kernels need to be recomputed as the underlying parameters change. Here $N = 2$, implying the observer gains are matrix-valued functions with $(N+1)^2 = 9$ components each, for a total of 18 individual functions for a given operating point.

In [14] the mean demand $C_W$ was fixed at $C_W = 6.25\ L/hr$ for the 50000 and 70000 consumers at the outlets of pipeline 1 and 2 respectively. As this in reality varies slowly throughout the day and year we wish here to see how the observer gains vary based on changing demand levels. The gains are calculated for 6 different operating points around this, namely $C_W \in \{1.67, 3.33, 5.00, 6.67, 8.33, 10.0\}$ $[L/hr]$. The resultant plots are shown in Figure 3, with Figure 3a showing the plots for $P_1$ and Figure 3b displaying $P_2$.

In most cases the observer gains increase in magnitude as the mean demand $C_W$ increases. There are a few exceptions for $P_1$ in Figure 3a, with the magnitude instead moving towards 0 as $C_W$ increases, this being due to the constant offset term $-F^{\alpha}L$ in (8a). Additionally, the gains corresponding to

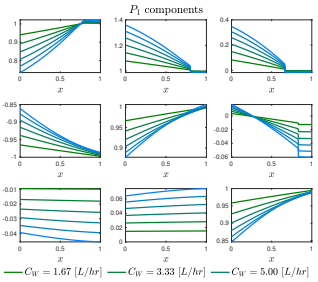


(a) Components of $P_1$ for various values of $C_W$.

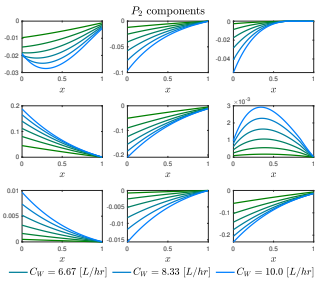


(b) Components of $P_2$ for various values of $C_W$.

Fig. 3: Observer gain matrix components, plotted as functions of $x \in (0,1)$ for values of mean water consumption $C_W$ between 1.67 $L/hr$ and 10.0 $L/hr$. Plots are organised as the individual components would appear in the respective matrix.

the three terms in the strictly upper triangular part of $P_1$ have discontinuities at $x = \frac{\lambda_i}{\lambda_j}$ for $0 \leq i < j \leq 2$ , this being a consequence of the kernel solution discontinuity drawn schematically in Figure 2.

## V. Conclusion

We have found the closed-form solution of observer backstepping kernel equations associated with a particular structure of $n+m$ linear hyperbolic PDEs for use in leak detection in branched pipe flows. This extends both the work of [14], where the leak detection method is derived, but also [12], which found the closed-form solutions of backstepping kernels for $2 \times 2$ linear hyperbolic PDEs with constant coefficients. Knowing these explicit kernel solutions is shown to facilitate the computation of numerically accurate observer gains with minimal computational effort, allowing the leak detection method from [14] to be implemented effectively in more realistic settings where the operating point is varying.

This being the first closed-form kernel solution for an $n+m$ linear hyperbolic PDE system with a specific structure, future work should investigate whether explicit solutions can be found for more general forms of such kernel equations. To complement the results in this paper, it should be investigated whether the kernel solutions for the case of leak detection in pipes connected in a loop, as considered in [15], can also be expressed analytically. Also, the results from this paper should be generalized to networks with multiple branching points, as opposed to a single branching point that is considered here.

## References


[1] K.-S. Son, S.-H. Jeon, Y.-C. Choi, and J.-W. Park, "Oil leak detection on a plant by using cctv camera," in *Proceedings of the Korean Society for Noise and Vibration Engineering Conference*. The Korean Society for Noise and Vibration Engineering, 2011, pp. 136–141.

[2] J. Chen, P. Tang, T. Rakstad, M. Patrick, and X. Zhou, "Augmenting a deep-learning algorithm with canal inspection knowledge for reliable water leak detection from multispectral satellite images," *Advanced Engineering Informatics*, vol. 46, p. 101161, 2020.

[3] F. Tanimola and D. Hill, "Distributed fibre optic sensors for pipeline protection," *Journal of Natural Gas Science and Engineering*, vol. 1, no. 4-5, pp. 134–143, 2009.

[4] Y. Yu, A. Safari, X. Niu, B. Drinkwater, and K. V. Horoshenkov, "Acoustic and ultrasonic techniques for defect detection and condition monitoring in water and sewerage pipes: A review," *Applied Acoustics*, vol. 183, p. 108282, 2021.

[5] C. Verde and L. Torres, *Modeling and monitoring of pipelines and networks*. Springer, 2017.

[6] L. Billmann and R. Isermann, "Leak detection methods for pipelines," *Automatica*, vol. 23, no. 3, pp. 381–385, 1987.

[7] C. Verde, "Multi-leak detection and isolation in fluid pipelines," *Control Engineering Practice*, vol. 9, no. 6, pp. 673–682, 2001.

[8] O. M. Aamo, J. Salvesen, and B. A. Foss, "Observer design using boundary injections for pipeline monitoring and leak detection," *IFAC Proceedings Volumes*, vol. 39, no. 2, pp. 53–58, 2006.

[9] O. M. Aamo, "Leak detection, size estimation and localization in pipe flows," *IEEE Transactions on Automatic Control*, vol. 61, no. 1, pp. 246–251, 2015.

[10] R. Vazquez, M. Krstic, and J.-M. Coron, "Backstepping boundary stabilization and state estimation of a $2\times$ 2 linear hyperbolic system," in *2011 50th IEEE conference on decision and control and european control conference*. IEEE, 2011, pp. 4937–4942.

[11] A. Smyshlyaev and M. Krstic, "Closed-form boundary state feedbacks for a class of 1-d partial integro-differential equations," *IEEE Transactions on Automatic Control*, vol. 49, no. 12, pp. 2185–2202, 2004.

[12] R. Vazquez and M. Krstic, "Marcum q-functions and explicit kernels for stabilization of $2\times$ 2 linear hyperbolic systems with constant coefficients," *Systems & Control Letters*, vol. 68, pp. 33–42, 2014.

[13] D. B. Saba, F. Bribiesca-Argomedo, J. Auriol, M. Di Loreto, and F. Di Meglio, "Stability analysis for a class of linear 2x2 hyperbolic pdes using a backstepping transform," *IEEE Transactions on Automatic Control*, vol. 65, no. 7, pp. 2941–2956, 2019.

[14] H. Anfinsen and O. M. Aamo, "Leak detection, size estimation and localization in branched pipe flows," *Automatica*, p. 110213, 2022.

[15] N. C. A. Wilhelmsen and O. M. Aamo, "Leak detection, size estimation and localization in water distribution networks containing loops," in *61st IEEE Conference on Decision and Control (CDC)*, 2022, pp. 5429–5436.

[16] D. R. Maidment and S.-P. Miaou, "Daily water use in nine cities," *Water Resources Research*, vol. 22, no. 6, pp. 845–851, 1986.

[17] N. C. A. Wilhelmsen and O. M. Aamo, "Distributed observer-based leak detection in pipe flow with nonlinear friction (extended abstract)," in *2nd IFAC Workshop on Control Methods for Water Resource Systems*, 2022.

[18] R. A. Bajura, "A model for flow distribution in manifolds," *Journal of Engineering for Power*, vol. 93, no. 1, pp. 7–12, 1971.

[19] F. Branin, "Transient analysis of lossless transmission lines," *Proceedings of the IEEE*, vol. 55, no. 11, pp. 2012–2013, 1967.

[20] A. Aw and M. Rascle, "Resurrection of" second order" models of traffic flow," *SIAM journal on applied mathematics*, vol. 60, no. 3, pp. 916–938, 2000.

[21] L. Hu, F. Di Meglio, R. Vazquez, and M. Krstic, "Control of homodirectional and general heterodirectional linear coupled hyperbolic pdes," *IEEE Transactions on Automatic Control*, vol. 61, no. 11, pp. 3301–3314, 2015.

[22] M. Abramowitz and I. A. Stegun, *Handbook of mathematical functions with formulas, graphs, and mathematical tables*. US Government printing office, 1964, vol. 55.